ABSTRACT

Modeling has always been an integral part of the study related to electronic devices. It helps in better understanding the theory and analyzing the characteristics related to the electronic devices. One such electronic device is enzyme field effect transistor (ENFET), popularly used as biosensor or point of care (POC) device. This device is an applied innovation in the field of device technology involving biological, chemical and electronic principles. This thesis aims at electrochemical modeling and validation of high-κ dielectric and nanomaterial based ENFETs for biomolecule detection.

In the first work, the key steps involved in electrochemical modeling of high-κ dielectric and nanomaterial based ENFETs have been formulated based on the study on modeling of ENFETs with special emphasis on nanomaterial based ENFETs with high-κ dielectrics as insulator. The modeling has been carried out considering the enzymatic reactions, diffusion phenomena of substrate and products in the electrolyte, acid/base reactions of the product in the electrolyte, pH detection properties and the current transport model of nanomaterial based ENFET device. Using the key steps, a generalized electrochemical model for nanomaterial based ENFETs has been reported.

In the second work, the validation of the developed model has been carried out using graphene based ENFET (G-ENFET) with ZrO_2 as dielectric for cholesterol detection. The variations in the traditional model due to use of graphene as substrate has been discussed. The insulating layer of high-κ dielectric, ZrO_2 has shown good insulating effect even at nanometer range. The mobility of graphene is very high, which contributes towards the high sensitivity of the device as even very small potential variation at the surface gives a noticeable change in current. For comparison of modeling results with the experimental results, different parameters have been used i.e. surface potential, threshold voltage, drain current and device sensitivity. The modeling results for all the three devices have been found to be in good agreement with the experimental results with respect to all the parameters.

In the third work, the validation of the developed model has been carried out using carbon nanotube based ENFET (CNT-ENFET) with ZrO_2 as dielectric for acetylcholine detection. The variations in the traditional model due to use of CNT as substrate has been discussed. CNT substrate makes the ENFET junctionless. The channel is already present along with source and drain so, the channel inversion potential required in traditional Si-based ENFET devices has been excluded in this device model. Moreover, due to high mobility of CNT, a good amount of current has been obtained at this nano level. The results based on the proposed model have been found to be in good agreement with the experimental results.

In the fourth work, the validation of the developed model has been carried out using CNT based dual gated ENFET (CNT-DG-ENFET) with HfO_2 as dielectric for acetylcholine detection. The variations in the traditional model due to use of dual gate have been discussed. HfO_2 is a high-κ dielectric with dielectric constant 25 and has thickness of about 10 nm in the fabricated device giving good insulating effect and enhanced sensitivity even at nanometer range. The use of ZnO, a low-κ dielectric, as the bottom gate material gives lesser current as compared to the top gate. Because of this, the variation in current mostly occurs because of top gate. The increase in sensitivity of the device to 1.1 V/pH, which is much higher than Nernstian limit (59 mV/pH) obtained using dual gate has been emphasized.

Graphically, the abstract for the three works has been represented by the following figures and graphs. Fig. 1 represents the general structure of high-κ dielectric nanomaterial based ENFET device. Fig. 2 represents the G-ENFET structure and its validated output characteristics. Fig. 3 represents the CNT-ENFET structure and its validated output characteristics. Fig. 4 represents the CNT-DG-ENFET structure and its validated output characteristics.

Graphical Abstract

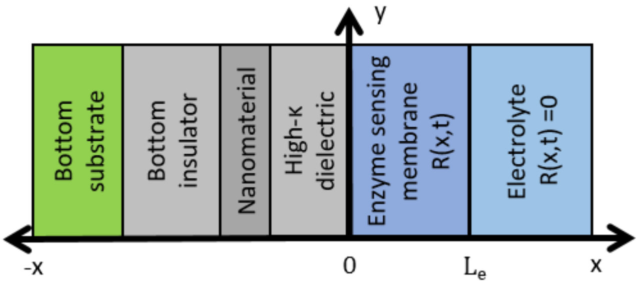

Fig. 1.

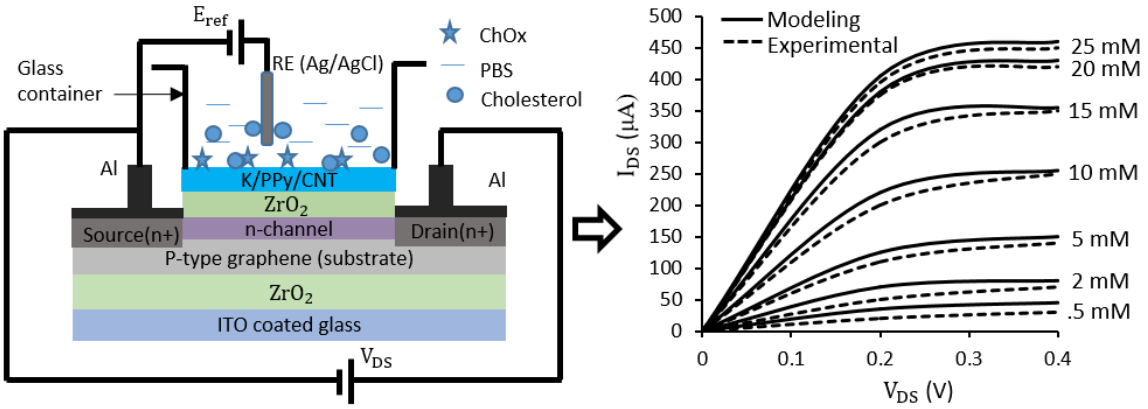

Fig. 2.

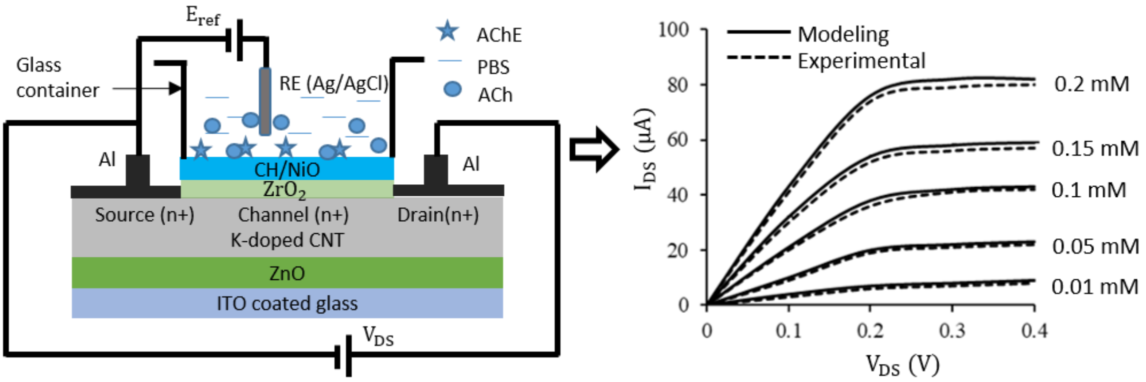

Fig. 3.

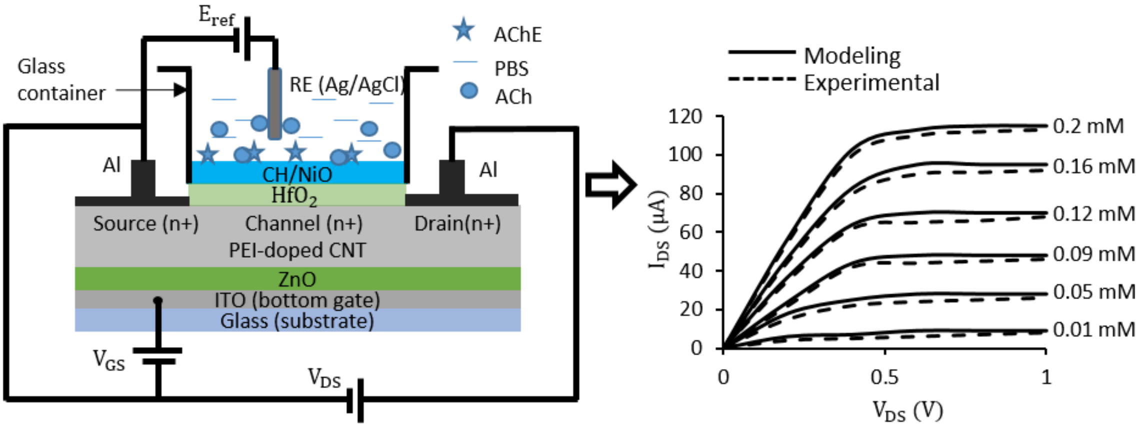

Fig. 4.